



## Article

# Reconstruction of Seasonal Kinetics in Conifer Radial Growth from Daily Meteorological Conditions, Tree-Ring Width, and Radial Size of Tracheids

Grigory K. Zelenov<sup>1</sup>, Liliana V. Belokopytova<sup>1,2,\*</sup> , Elena A. Babushkina<sup>1,2</sup> , Dina F. Zhirnova<sup>1,2</sup>, Bao Yang<sup>3</sup>, Xiaomei Peng<sup>4</sup>, Jingjing Liu<sup>4</sup>, Gleb A. Sitnikov<sup>5</sup> and Eugene A. Vaganov<sup>1,6</sup>

<sup>1</sup> Institute of Ecology and Geography, Siberian Federal University, 660041 Krasnoyarsk, Russia; zelenov.grigory@yandex.ru (G.K.Z.); babushkina70@mail.ru (E.A.B.); dina-zhirnova@mail.ru (D.F.Z.); eavaganov@hotmail.com (E.A.V.)

<sup>2</sup> Khakass Technical Institute, Siberian Federal University, 655017 Abakan, Russia

<sup>3</sup> School of Geography and Ocean Science, Nanjing University, Nanjing 210023, China; yangbao@lzb.ac.cn or yangbao@nju.edu.cn

<sup>4</sup> Key Laboratory of Desert and Desertification, Northwest Institute of Eco-Environment and Resources, Chinese Academy of Sciences, Lanzhou 730000, China; pxmphd@163.com (X.P.); liujj@lzb.ac.cn (J.L.)

<sup>5</sup> Independent Researcher, 655017 Abakan, Russia; glebstandreevich@gmail.com

<sup>6</sup> Department of Dendroecology, V.N. Sukachev Institute of Forest, Siberian Branch of the Russian Academy of Science, 660036 Krasnoyarsk, Russia

\* Correspondence: white\_lili@mail.ru

**Abstract:** The development of the tree ring is a process occurring under limitations caused by a complex of environmental factors and intrinsic regulatory mechanisms. Its understanding is of interest in many scientific fields, but most quantitative models trying to describe its details meet several issues stemming from the difficulty of its verification. This study attempted to combine several observational and modeling approaches to verify intermediate details of the description of xylogenesis, aiming to restore the tree-ring seasonal growth kinetics on the basis of dendrochronological and wood anatomical data. It was carried out for Scots pine in two semiarid habitats in South Siberia. The Vaganov-Shashkin model was used jointly with tree-ring width chronology and climatic data to model the tree radial growth rate with daily precision. The Band-model was then used to calculate the kinetics of tracheid production from the growth rate and actual final number of cells per radial file in the ring. Seasonal observations of cell population and final measurements of cell sizes were used to fit model parameters and verify the numbers of developing tracheids produced by the Band-model. The patterns of modeled seasonal kinetics for six seasons and two sites were found to repeat the actual drought-derived deviations in tree growth and observations ( $R^2 = 0.70\text{--}0.84$ ). Further research is required to test other climatic limitations and species-specific ecophysiological mechanisms of growth regulation.

**Keywords:** conifers; wood formation; seasonal kinetics of xylogenesis; tracheids; imitation modeling; Vaganov-Shashkin model; Band-model of xylogenesis



**Citation:** Zelenov, G.K.;

Belokopytova, L.V.; Babushkina, E.A.; Zhirnova, D.F.; Yang, B.; Peng, X.; Liu, J.; Sitnikov, G.A.; Vaganov, E.A.

Reconstruction of Seasonal Kinetics in Conifer Radial Growth from Daily Meteorological Conditions, Tree-Ring Width, and Radial Size of Tracheids. *Forests* **2024**, *15*, 249. <https://doi.org/10.3390/f15020249>

Academic Editors: Angela Balzano, Maks Merela and Veronica De Micco

Received: 10 January 2024

Revised: 24 January 2024

Accepted: 26 January 2024

Published: 28 January 2024



**Copyright:** © 2024 by the authors. Licensee MDPI, Basel, Switzerland. This article is an open access article distributed under the terms and conditions of the Creative Commons Attribution (CC BY) license (<https://creativecommons.org/licenses/by/4.0/>).

## 1. Introduction

Each tree ring formed in the trunk of a conifer tree differs in linear dimensions (width) and anatomical structure, both between trees and between years. These differences are the result of the seasonal kinetics of cell production by the cambium and subsequent differentiation processes of cell growth by expansion and secondary cell-wall thickening [1–6]. The processes of cell production and differentiation are under the control of internal (hormonal, like auxin, cytokinin, gibberellin, etc.) and external factors (mainly heat, moisture, nutrients, and light) [7–12]. Such control significantly complicates the quantitative description of the tree ring formation during the season, although several models and corresponding

algorithms have been proposed in the literature ([13–20]; see review [21]). Unfortunately, those models, with rare exceptions (e.g., the VS model), have not been widely used [21]. In our opinion, the main obstacles to the use of tree-ring-formation models presented in the literature are the following two factors: (1) a large number of model parameters cannot be measured experimentally; (2) it is often impossible to verify the intermediate steps of the model algorithm. However, original comparisons of the kinetics of tracheid seasonal formation and the developed structure of tree rings made it possible to assert that kinetics (the set of growth processes, described as time series of tracheid numbers and their traits at consequent differentiation stages, or as a sequence of durations for each stage and the rates of change in respective cell measurements from the total ring scale down to individual cells) explains the features of the tree-ring structure in conifers [14]. In this study, we attempted to solve the inverse problem using the chronologies and tracheidograms of tree rings to restore the kinetics of the seasonal growth of the tree ring.

We recently published a study in which the VS model was combined with the so-called Band-model of cambial activity. In the latter model, the number of parameters is sharply reduced, while the description of cell production by the cambium is still maintained [22]. In the current work, we expanded the possibilities of modeling the process of the anatomical structure in the tree ring, using direct measurements of the radial sizes of cells (tracheids) to describe and verify the process of their expansion after production by the cambium. Not being able to significantly reduce the number of parameters, in this work we tried to eliminate the second obstacle, making intermediate testing of the model possible. To do this, the analysis scheme relied on the following sets of input data: (1) daily series of precipitation and temperature (input variables for calculating radial growth rate in the VS model [2]); (2) tree-ring width chronologies developed for the study sites (to parameterize the VS model and assess its adequacy); (3) intra-seasonal observations of cell number in the expansion zone using periodic sampling from tree trunks [6]; (4) tracheidograms (intra-seasonal variability in cell radial sizes in the tree ring), averaged for five radial rows of cells [9,10,23], measured on the last samples collected over the seasonal growth kinetics observations. The main goal of this work was to reconstruct the growth kinetics of tree rings with the external block of the VS-model and Band-model, using experimental observations to verify the calculated data on the cell number per radial row in the ring and the radial diameters of the developed tracheids.

## 2. Materials and Methods

### 2.1. General Scheme of Analysis

The general calculation scheme used in this study is shown in Figure 1. In the first stage, the external block of the VS-model is applied (Figure 1a), where the input variables for calculating the growth rate are the daily climate data [2,24,25]. The adequacy of the estimation of the model parameter values was checked by comparing the modeled tree growth series with long-term tree-ring chronologies obtained for the selected sites (Figure 1b) using the following statistics: the correlation and synchronicity of the calculated growth rate with tree-ring width indices, and the root mean square error [19]. The results of the first stage are the VS-model parameters and seasonal kinetics of the relative cell production rate (Figure 1c) for each year, generalized for all tree rings formed in the corresponding years.

However, in the same year, different numbers of cells are produced in the rings of different trees, or even along different radii of the same trunk, depending on the individual characteristics of the tree, local growth conditions, competition, etc. Therefore, at the next stage, it is important to convert the integral rate of seasonal growth, common for a given year, into absolute rates of cell production in accordance with the average number of tracheids in the ring for a particular year in a particular tree. For this transformation, the Band-model was used (Figure 1d), with the help of which the relative growth rate was transformed into the dates of entry of each subsequent cell into the expansion zone, in accordance with the total cell production ( $N$ ) in a given tree ring (Figure 1e). At the final

stage of the calculations, measurements of tracheidograms (the final radial size of each cell) and theoretical (calculated) kinetics of expansion of each cell, described by an exponential curve, were used. In accordance with the date of entry of each cell into the expansion zone, determined by the Band-model, and the duration of their stay in this zone, stretching occurs simultaneously for several cells. Counts of their numbers using these models were compared with those measured periodically on cross-sections of wood samples collected throughout the season (Figure 1f).

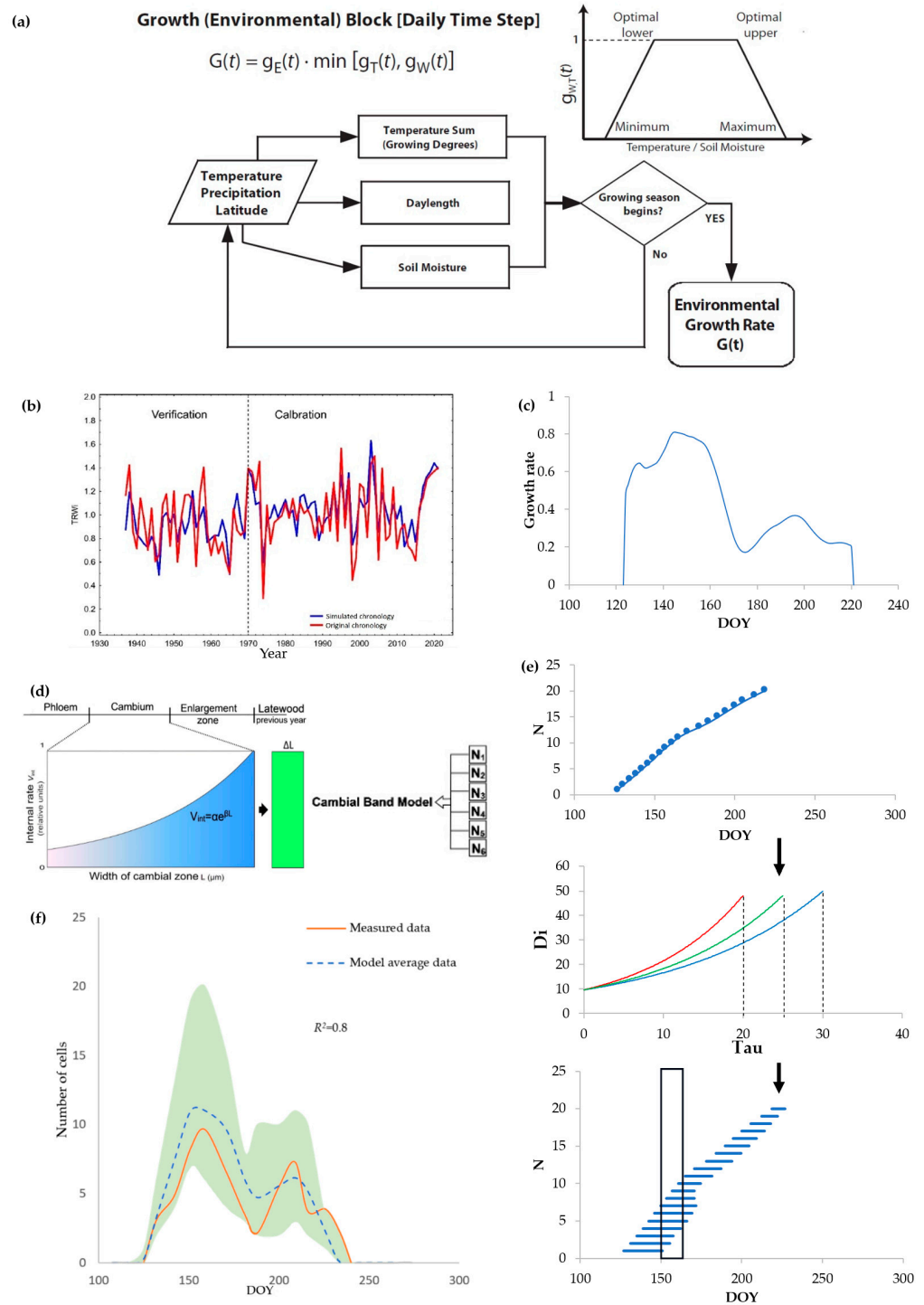


**Figure 1.** General scheme of analysis and representation of results: (a) Vaganov-Shashkin model, environmental block. Daily growth rates due to the environment are determined by comparing daily

temperature and soil moisture (calculated from temperature, precipitation, evapotranspiration, and soil drainage) to piecewise linear approximations of parabolic growth functions (inset). Partial growth rates caused by temperature  $g_T(t)$ , soil moisture  $g_W(t)$ , and solar radiation, estimated from daylength  $g_E(t)$ , are combined to calculate general growth rate  $G(t)$ . Adapted from [25]; (b) comparison of simulated tree-ring width index based on the seasonal sum of growth rate  $G(t)$  with standardized actual tree-ring width chronology in the VS-oscilloscope implementation [24]. Values of model parameters are fitted for the calibration period; then, the fitness of the model is tested for the verification period; (c) example of the calculated seasonal dynamics for general growth rate; (d) Band-model to produce seasonal growth curve (integral) according to different cell production rates in rings of different trees; (e) calculation of simulated cell number ( $N$ ) in the expansion zone during the season: example of the growth curve for a particular tree ring (the dates of cells' transition to the zone of expansion); curves which show the expansion of cell diameter ( $D_i$ ) according to its different possible rates (high – red line, middle – green line, and slow – blue line) used to calculate the duration of expansion ( $\tau$ ) for cells of a particular radial size; growth curve of  $N$  combined with intervals of each cell expansion, and 5-day window (black box) for counting cells in the expansion zone; sequence of calculations is shown with black arrows; (f) final comparison of the modeled and measured cell numbers in an expansion zone for a particular year (for example, the average data from analyzed trees for a particular year). Intra-seasonal timeframe on the horizontal axis is represented as day of year (DOY).

## 2.2. Sampling Sites Description

The study was carried out in the Khakass–Minusinsk Depression, a vast intermountain valley in the basin of the Yenisei River, South Siberia, Russia (Figure 2). This region has a sharply continental climate and receives an annual precipitation of approximately 350 mm based on the data obtained from Minusinsk weather station ( $53^{\circ}41' N$   $91^{\circ}40' E$ , 250 m a.s.l., 1936–2021). Two sites were chosen to perform the following types of wood sampling from Scots pine (*Pinus sylvestris* L.): (1) cores from at least 20 trees to build long-term tree-ring width chronologies (see, e.g., [10,19] and references there for previous research in the study area); (2) repeated small samples from 5–10 trees (selected separately each year) over the warm season to observe the seasonal growth kinetics.



Figure 2. Cont.



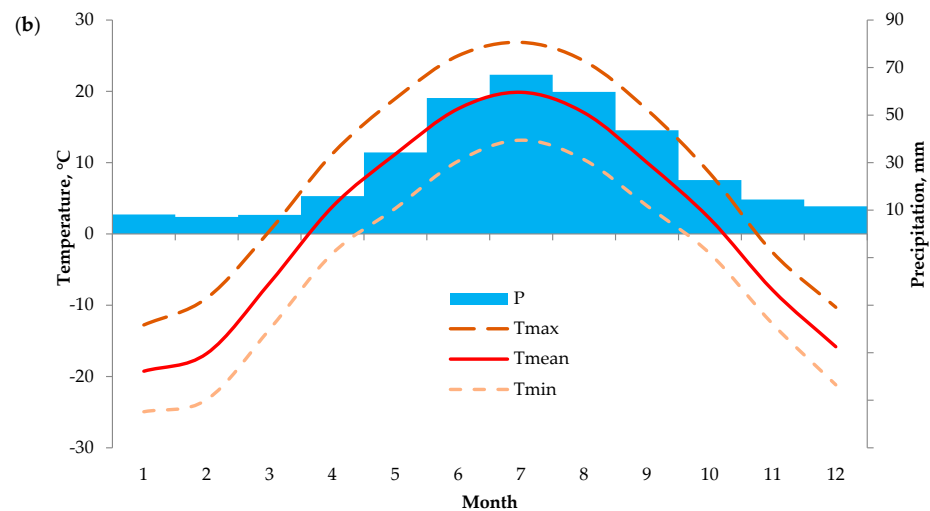


**Figure 2.** The study area: (a) satellite map (©Google) with marked locations of the sampling sites (circles) and the Minusinsk weather station (triangle); years of sampling are shown next to sampling site codes BID and MIN; map was modified from [26]; (b) climatic diagram of the Minusinsk weather station (1936–2021): monthly precipitation (P, bars), maximum (Tmax, dark dashed line), mean (Tmean, solid line), and minimum (Tmin, light dashed line) temperatures.

These are the basic characteristics of the studied sites: (1) the uneven-aged, isolated pine forest within the steppe zone near Minusinsk city (MIN; 2013, 2014 and 2017— $53^{\circ}39' N$   $91^{\circ}36' E$ , 320 m a.s.l.; 2021— $53^{\circ}40' N$   $91^{\circ}42' E$ , 260 m a.s.l.); (2) the mixed forest consisting of pine, larch, and birch in the forest-steppe ecotone in the foothills of the Batenevsky Ridge, Kuznetsk Alatau Mountains, on the border of the Khakass–Minusinsk Depression, near the Vershino-Bidja village (BID; 2018, 2019— $54^{\circ}00' N$   $90^{\circ}59' E$ , 600–650 m a.s.l.). A short geobotanical description of the sites is presented in Table S1.

Daily climatic series of the closest Minusinsk weather station (1936–2021) and latitudes of the sampling sites were used as input data in the VS-model. Despite the substantial distance of Minusinsk station from Vershino-Bidja, its air temperature and precipitation series were found to be more appropriate in quality for dendroclimatic analysis at the BID site compared to Shira, the other available weather station located at a similar distance, due to the longer daily series and steady dendroclimatic correlations. The mountain ridge located between Shira station and the BID site and the flat valley spanning from BID to Minusinsk station probably contribute to the climate of that sampling site being more similar to the climate at Minusinsk station.

### 2.3. Long-Term Tree-Ring Width Chronology Development

To obtain tree-ring width (TRW) chronology, wood cores at each site were collected at breast height from the east or west direction using an increment borer from more than 20 healthy (without damage to trunk, branches, and foliage) and mature dominant and subdominant pine trees. Cores were processed using standard dendrochronological methods [27]. The tree-ring width was measured with an accuracy of 0.01 mm using the LINTAB5 measuring tool and the TSAPwin program (Rinntech, Heidelberg, Germany [28]). The accuracy of cross-dating individual TRW series with master chronology was verified using the COFECHA program [29]. Raw measurement series were indexed using exponential functions to estimate age-related trends, and the TRW index was calculated as the ratio of the actual value to the trend value [27]. The autocorrelation component was then also removed to highlight the climatic signal. Subsequently, residual TRW series were averaged within each site with the binomial weighted mean. The ARSTAN program [30] was used for indexing and generalization. The main statistical characteristics of the TRW site chronologies are presented in Table S1.

#### 2.4. Seasonal Growth Observations

To produce the seasonal growth kinetics observations, we selected 5–10 trees of *P. sylvestris* in the same place or similar places nearby, following the same principles as the sample collected for building the tree-ring width chronology. Samples were collected from mid-April to mid-September by extracting short cores of 2–3 growth rings, on average, at 10-day intervals. Samples were collected at a height of ca. 1.2–1.4 m on the southern half of the tree trunk surface in oblique rows ca. 5 cm apart. The collected cores were placed in a water–ethanol–glycerol solution (1:1:1) and stored at a temperature of ca. 6 °C. For each wood core, cross-sections of 14–16 µm thickness were prepared using a rotary microtome Microm HM340E (Thermo Fisher Scientific, Waltham, MA, USA). Cross-sections were stained with safranin and Astra blue pigments (1% water solutions, 1:1) to distinguish lignified (stained magenta) tissue from non-lignified (stained blue) tissue. Microphotographs of cross-sections were taken at 200× magnification using a digital camera ProgRes Gryphax Subra (Jenoptik GmbH, Leipzig, Germany) mounted on a biological microscope BX43 (Olympus, Tokyo, Japan). In each microphotograph, cells in the expansion zone were recognized as cells larger than those in the cambial zone (the smallest and the most thin-walled) but without signs of cell-wall thickening and lignification (color change from blue to magenta), and expanding cells were counted and averaged over five radial rows of tracheids (see [6] for more details). To estimate the variability in cell numbers, we calculated the standard error (*SE*) of the mean values for the five measured radial rows.

#### 2.5. Measurement of Tracheidograms

The last samples collected at the end of the season (the second half of September), and the cross-sections of wood prepared from them, were used to measure tracheidograms averaged over five rows of cells [10,23]. Tracheidograms were a sequence of radial sizes measured for cells in the direction from the inner boundary of the tree ring (beginning of seasonal growth) to the outer boundary (end of the season). Typical examples of tracheidograms for the study area can be seen in earlier publications by the authors [1,2,9,10]. Measurements were made on photographs of cross-sections obtained in the same way as for observation of seasonal kinetics. For subsequent analysis, it was assumed that each subsequent cell in the row was produced by the cambium after the previous one, and the cells also sequentially transitioned to the expansion zone. Thus, we eliminated the possibility of 2–4 cells transitioning from the cambial zone to the expansion zone at a time, although experimental grounds for such a hypothesis exist [31,32].

#### 2.6. Simulation of Tree-Ring Width Chronologies and Calculations of Seasonal General Growth Rate

The complete description of the VS-model is well presented in several publications [2,19,25]. To evaluate the model parameters, we used a VS oscilloscope implementation, which allowed for us to describe the piecewise linear trapezoidal functions of the growth rate dependences on soil moisture (estimated using temperature, precipitation, evapotranspiration, and drainage losses) and air temperature [24]. The model assumes that three key environmental variables influence seasonal radial growth: solar radiation, air temperature, and moisture availability (Figure 1a). These three factors determine the daily rate of new xylem cell production (calculated general growth rate) using the principle of limiting factors. The onset of the growth season is determined by a specific threshold sum of temperatures for the previous short period, which is usually 60–100 degree-days over 10–12 days (Table 7.2 in [2]; cf. critical temperatures 5–8 °C required for the onset of xylogenesis of boreal conifers described in [33]). A more detailed description of the growth rate calculation is presented in [2] (pp. 211–214).

In addition, the input data for the VS-model included parameters depending on the tree species and growing conditions (Table 7.2 in [2]). Interactive work with the VS-oscilloscope made it possible to determine the model parameter values that most accurately describe the dynamics of the radial growth indices based on the obtained long-term series. The quality of the modeling was checked by dividing the initial TRW chronology into

two temporal intervals, one of which was used for calibration and the other for verification. To assess the quality of the modeling, the following statistical indicators were used: correlation coefficient (R), synchronicity coefficient (Glk), and root mean standard error (RMSE) [34].

### 2.7. Usage of Band Model

Calculations using the VS model ultimately made it possible for each year to obtain the intra-seasonal dynamics of the general growth rate (production) in relative values. This is a generalized calculated characteristic of the influence of external conditions on growth and tree-ring formation for all trees in the studied forest stand/species in a specific growth year. However, the seasonal growth measurements involved 5–7 trees, which produced different numbers of cells (and different tree-ring widths) in the year of observation (Table S2). To connect the seasonal growth kinetics and the final number of cells in the radial row for the ring of a particular year in a particular tree, a band model was used. As shown earlier [22], the key parameters of the model are the coefficients  $\alpha$  and  $\beta$ . Coefficient  $\alpha$  is obtained from estimates of the minimum growth rate (the rate of division of the initial), and coefficient  $\beta$  determines the heterogeneity of growth within the cambial zone. The time between the production of successive cells during a season was estimated by achieving a “band” production of 10  $\mu\text{m}$  (the average radial size of cells in the cambial zone), i.e., this nominal size of the cell leaving the cambial zone is the ratio between the theoretical “band” production, measured in  $\mu\text{m}$ , and the actual production, measured in cell number. Using a sequential iterative procedure, we selected a value of  $\beta$  that, when summing up the daily rates of “band” production, ultimately gave the value of the number of cells for a particular year and tree. The result of the calculations is the date when each consecutive cell in the measured tracheidogram enters the expansion zone. Note also that it was previously shown that the more cells were produced per season, the shorter the time intervals between them in terms of the time when they enter the expansion zone, and the lower the value of  $\beta$  [22].

### 2.8. Description of Cell Expansion Kinetics

After leaving the cambial zone, the cells expand in the radial direction to their final size, as recorded in the tracheidogram of the formed tree ring at the end of September. Describing the growth rate of the cambial “band” as an exponential, we assumed that, in the expansion zone, the cells will grow according to an exponential law (Figure 1e). At this stage of constructing the quantitative kinetics of growth ring formation, we assumed that the exponential function is determined in a simple way: the cell reaches a size of 50  $\mu\text{m}$  within 20–30 days. Similar estimates have been provided in experimental studies of tracheids in the growth rings of pine and spruce [1,35,36]. Naturally, if the final cell size is smaller, then the time of expansion is also shorter, and for latewood (cell size 12–20  $\mu\text{m}$ ) it is only 5–7 days [35]. Note that the term of the exponent can be constant for a particular year and individual tree, but it can also change depending on the current conditions during the expansion process, for example, when turgor decreases [37].

## 3. Results

### 3.1. Fitting of VS-Model Parameters for Chronologies and Calculation of Seasonal Growth Rate

The modeled and actual chronologies of tree-ring width indices for two sampling sites of seasonal growth kinetics observations are shown in Figure S1, and the fitted parameters and statistics of the VS-model are presented in Table S3. The correlation and synchronicity values indicate a satisfactory agreement between the simulated and experimental data. It is interesting to note that the model parameters fitted using a VS-oscilloscope indicate differences in the soil conditions of the two forest stands. The parameters of the temperature response do not contradict the faster achievement of the maximum at the BID site because the stony soil contributes to the rapid heating of its upper layer. This also explains the lower value of the sum of temperatures for the start of growth processes in the season

under these soil conditions. It is also obvious that in sandy soil conditions, roots reach greater depths than in the area with stone inclusions. Small differences are also noted in moisture loss during transpiration; pines on stony soil transpire more than those on sandy soil. This is again due to the better heating of the top layer of soil, while in sandy soil conditions, moisture has to be lifted from the lower layers of soil where it is infiltrated.

The calculated general rates of seasonal growth (cell production) are shown in Figure 3a for the years when the seasonal kinetics of tree-ring growth were observed by periodic sampling during the season. It is easy to see that the beginning and end of cell production vary in accordance with the current climatic conditions of individual years. In addition, the conditions of the year of growth determine the achievement of a relative maximum of production (clearly visible when comparing, for example, 2018 and 2019). In 2013 and 2017, there was bimodality in the rate of wood production.

### 3.2. Band-Model: Absolute Production of Tracheids and Dates of Tracheid Transition from Cambium to Expansion Zone

For each specific year, The VS-model estimates the tree growth rate, limited by temperature, soil moisture, or insolation (day length). This general growth rate is the same for all trees in the studied forest stand and is expressed in relative units. However, we performed measurements for specific trees, with a specific absolute radial growth (tree-ring width). This is especially true for seasonal measurements, which summarize the data measured on several trees. Conversion of the single calculated growth rate resulting from the VS-model into the kinetics of cell production in different trees within the site (trees of different growth energies, ages, etc.) using the Band-model, we obtained the following results:

- For growth rings of different widths (and different numbers of tracheids in radial cell rows), we were able to calculate the seasonal kinetics of growth in terms of the number of cells in the ring.
- For each tracheid in the cell row, we determined the date of its production by the cambial zone (i.e., the date of transition to the expansion zone).
- The inverse relationship between the number of produced cells and the main parameter of the Band-model ( $\beta$ ) is clearly evident.

The good convergence of the model results with the actual kinetics of the number of expanding tracheids, both for individual years of observations and for the entire dataset as a whole, is ensured by the exponential approximating functions with a negative coefficient for the parameter  $\beta$  (Table 1).

**Table 1.** Equations for the relationship between the number of produced cells (N) and the main parameter of the Band-model ( $\beta$ ). Numerical terms were selected on the basis of comparison between the experimentally obtained and calculated numbers of expanding cells.

Year	Equation
2013	$N = 92.6 \cdot \exp(-1.096 \cdot \beta)$
2014	$N = 106.4 \cdot \exp(-1.37 \cdot \beta)$
2017	$N = 77.0 \cdot \exp(-0.97 \cdot \beta)$
2018	$N = 108.0 \cdot \exp(-1.22 \cdot \beta)$
2019	$N = 105.1 \cdot \exp(-1.11 \cdot \beta)$
2021	$N = 104.3 \cdot \exp(-1.31 \cdot \beta)$
Total	$N = 95.0 \cdot \exp(-1.1 \cdot \beta)$

Note that the maximum value of cell number N varies from year to year, which indicates the influence of current climatic conditions on the realization of growth potential. Simultaneously, in years with suppressed growth rates within the season (2013 and 2017), the value of the maximum possible cell production per season also noticeably decreases.



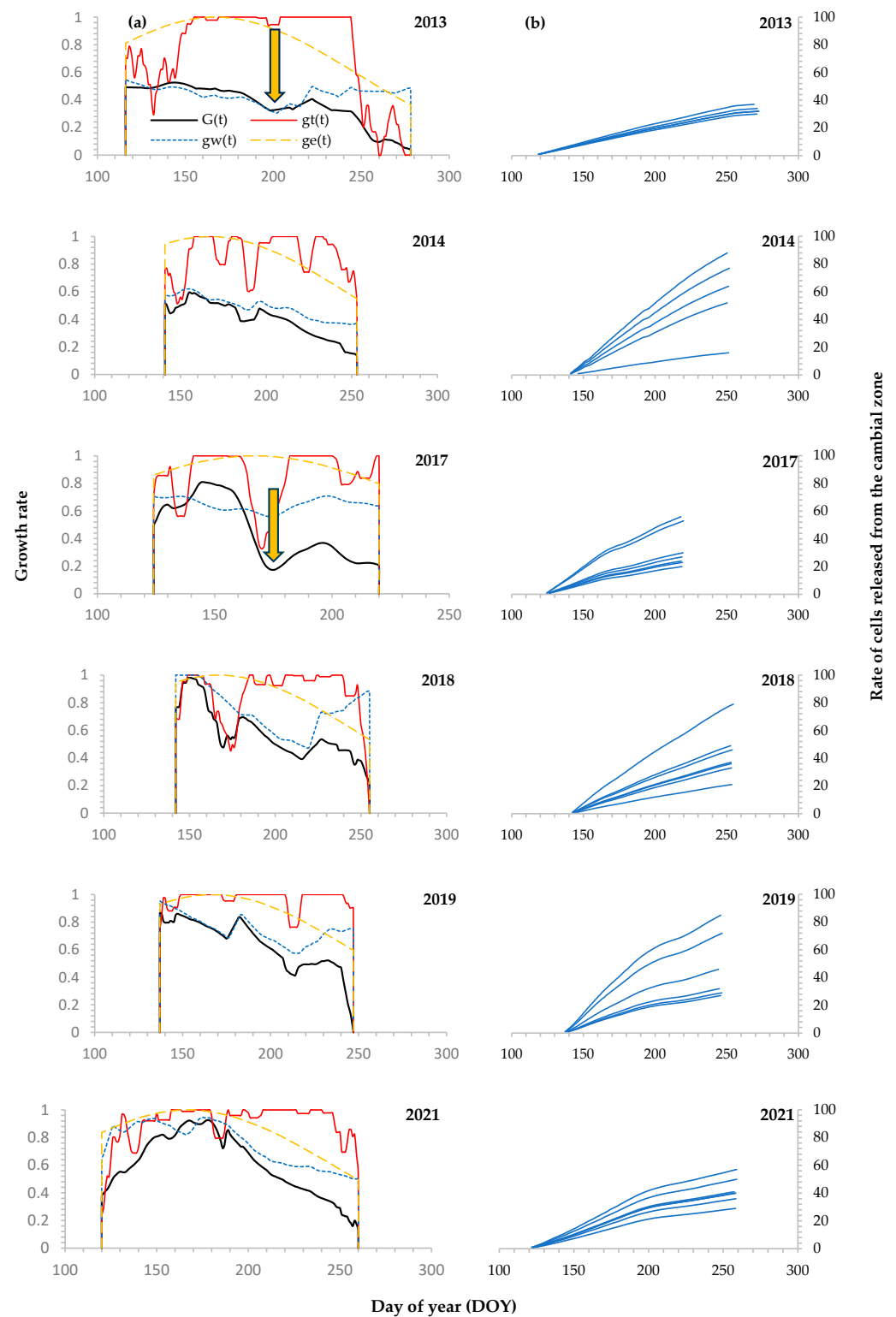


**Figure 3.** Modeled and actual seasonal kinetics: (a) calculated using the VS model daily general growth rates of tree growth  $G(t)$  and partial growth rates caused by temperature  $g_T(t)$ , by soil moisture  $g_W(t)$ , and by the solar radiation estimated from daylength  $g_E(t)$ ; arrows mark bimodal growth; (b) actual increase in the number (production) of cells (dates of each cell transition into expansion zone) in the tree ring for all observed trees/years.

### 3.3. Cell Production Kinetics

The calculated kinetics of the produced cell number  $\tau$  using the Band-model for tree rings formed in observed trees/years are shown in Figure 3b. Since the kinetics calculations within the year are based on the same rate of production for all trees (Figure 3a), the  $\tau$  curves for trees with different final production levels are similar and can easily be scaled to each other. Between years, curves differ in the timing of the beginning and end of cambial activity, but the general trend is a slightly higher rate of cell production in the first half of the growth season, which is manifested less for tree rings with a relatively small number of formed cells ( $\leq 30$ ). In 2017, a minimum clearly appeared on the curves in the active part of the season (late June–early July), but in 2013, a similar minimum was less significant due to the smaller number of cells that were produced during the season. The nature of these minima in the production rate, as shown in a previous study [6], is a strong local intra-seasonal drought, when the average and maximum temperatures reach a maximum, and the precipitation of the previous period does not provide a sufficient water balance (Figure S2). Such a reaction is consistent with the dendroclimatic relationships in the study regions reported earlier [6,10,19]. It is possible to note some features of individual years in the kinetics of production rates, e.g., a slowdown in rate was clearly evident in the middle of the season in 2017, and in the final stage of the growth season (in August) in 2019. In 2021, a rather sharp difference between the first and second half of the growth season was observed.

### 3.4. Analysis of Tree-Ring Tracheidograms at the End of the Growth Season

To calculate the number of cells in the expansion zone according to the general analysis scheme (Figure 1), it was necessary to measure the tracheidograms of the studied tree rings [2,38,39]. In Figure 4, all actual (measured) tracheidograms, in accordance with the number of cells for each individual tree at the end of the season, are shown on the left, and on the right, the tracheidograms normalized to the average number of cells in the measured tree rings within a particular year can be seen.

It can be noted that, despite the different final numbers of cells between trees in a season, their normalized tracheidograms show an enviable similarity. This is manifested not only in the values of the cell radial size, but also in the signature features of intra-seasonal curves. For example, all tracheidograms in 2013 clearly show an intra-seasonal fluctuation, a “false ring” (intra-annual density fluctuation, IADF); in 2014, there is a consistent decrease in the cell radial size from the beginning of the season to its end; an increase in the cell radial size in the first half of the season (earlywood), and then a decrease in size in transition wood and latewood, occurred in 2019; the tracheidograms in 2021 clearly highlight a zone of large cells and then a sharp transition to small latewood cells. An interesting example was observed in 2017: of the seven measured trees during the season, the two widest rings with a cell number exceeding 50 showed a clear intra-seasonal suppression of radial cell size, with the number of cells produced before and after this event being approximately equal (about 28 cells), while the other five trees (with an average of 25 cells) showed a sharp decrease in the cell radial size after the production of 17 cells, after which no more than 8 cells were formed. A comparison of climatic diagrams, calculated growth rate curves, and tracheidograms of tree rings with pronounced false rings (2013 and 2017) shows that this phenomenon occurred at the end of the first decade of July, in 2013, and at the beginning of the last decade of June in 2017 (Figure S2). In the latter case, the effect was more significant and inhibited cell production in five slow-growing trees compared with fast-growing ones.

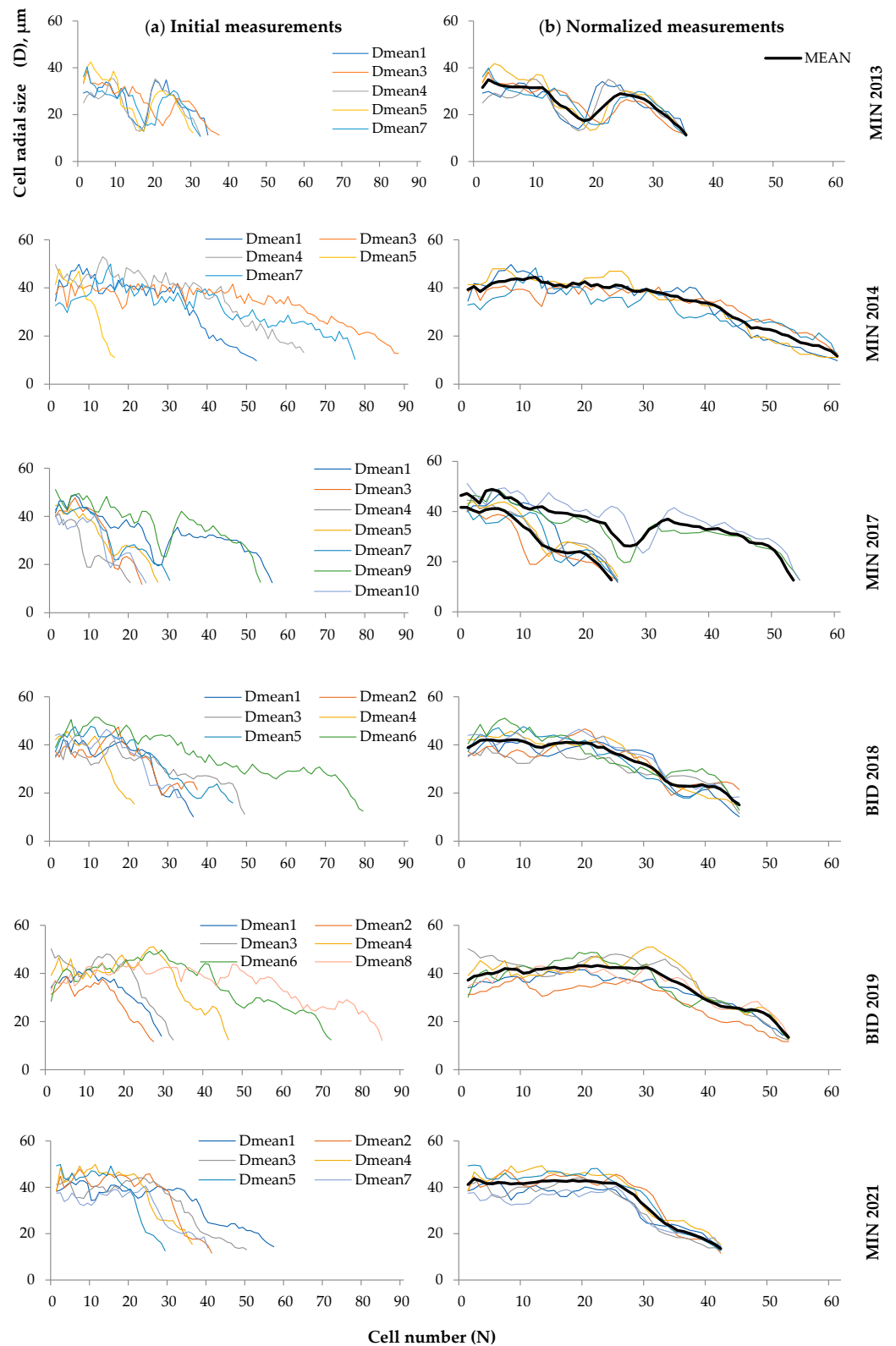


**Figure 4.** Tracheidograms of cell final radial size at the end of September within tree rings for years of seasonal kinetics observations: (a) measured tracheidograms averaged over five radial rows for each tree; (b) tracheidograms after being normalized to the average number of cells for all experimental trees during a particular year, as well as their mean. Note that, in 2017, distinctive patterns were observed in fast- and slow-growing trees, as demonstrated on normalized tracheidograms.

### 3.5. Seasonal Curves of the Number of Cells in the Expansion Zone

Measurement of tracheidograms resulted in expansion times for each cell in sequence from the inner to the outer border of the tree ring, consistent with the assumption of an exponential curve of the final radial size of the tracheid according to the duration of its expansion (Figure 1e). In the calculations, a fixed final value was used as the maximum value of the radial size (50  $\mu\text{m}$ ). A comparison of the calculated and measured cell numbers in the expansion zone during the season was carried out for the duration of the expansion to this maximum size of 20, 25, and 30 days, and the greatest fitness was observed when using the 30-day option in the calculations (Figure 5). Naturally, each cell in the measured tracheidogram had a specific radial size value, so the duration of expansion varied from 25–28 days for earlywood cells to 5–7 days for the smallest latewood cells. A high similarity between the measured and calculated curves was observed ( $R^2 = 0.70\text{--}0.84$ ), as well as the repetition of the signature features of the measured curves in those calculated, for example, the bimodality in 2013 and 2017.

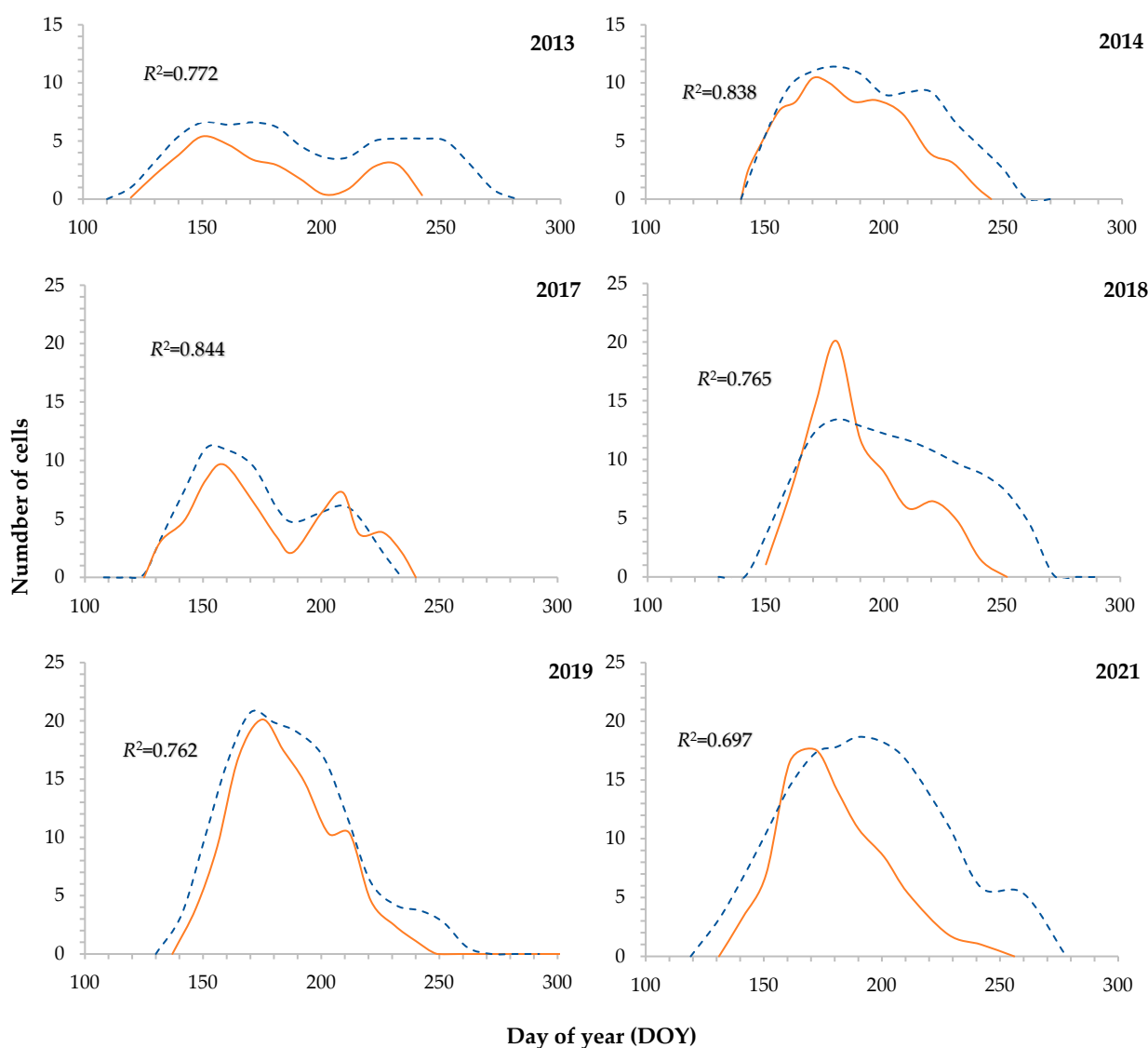


**Figure 5.** Measured and calculated cell numbers in the expansion zone (averaged data for several trees) in the years of seasonal growth kinetics observations. Orange solid lines represent measured data; blue dashed lines represent calculated data (there are more data points in calculated data due to the use of all cells in the tracheidograms).

#### 4. Discussion

If the seasonal growth kinetics largely explains the features of the tree-ring structure [14], then the above data can be interpreted as a solution to the inverse problem, i.e., the final structure of tree rings can be used to reconstruct the features of the seasonal growth kinetics. It is obvious that the influence of external conditions is significantly reflected in the tree-ring structure. Each of the produced rings has its own particular anatomical structure, which can be assessed through the quantitative characteristics of tracheidograms [5,9,40,41]. Solving the direct (influence of climatic factors on the growth kinetics and tree-ring structure) and inverse problems is important in both fundamental and applied aspects. It is clear that a specific combination of the temperature and water availability characteristics of the season determines the specifics of the tracheidograms of radial cell size [2,25,42].

An important issue is the influence that the anatomical characteristics have on each other. In previous works, we repeatedly provided examples of significant relationships between anatomical characteristics in the sequence of the formation of each tracheid in a season [2,9,10]: cell production affects the radial size of tracheids (both average and maximum in the ring, as well as for separate cells), which, in turn, has a nonlinear relationship with cell wall thickness [2]. This relation implements a genetic program that can transform xylem cells into elements of the water supply and structural support system of a woody plant [43]. However, if the researcher has a good dataset on the measurements of the tree-ring formation's seasonal kinetics, then, by selecting the values of the parameters used in the above-described algorithm for reconstructing these kinetics and comparing them with the measured characteristics, it is possible to test simple hypotheses about the quantitative relationships between the production and expansion of cells. For example, to what extent is cell expansion determined by current water conditions (i.e., turgor [36]), and to what extent is cell expansion a legacy from the rate of their production [2,39]?

What does the reconstruction described above provide researchers? It is obvious that the duration of the series of growth kinetic reconstruction provided by our version is limited by the duration of the climatic series. However, we can use these existing climatic series, covering several decades (for example, up to 100 years), to classify them into a few typical climatic modes (patterns of meteorological conditions and extreme events occurring repeatedly over several years during the cover period) for the study area, and then recognize corresponding patterns in the reconstructed curves of the growth seasonal kinetics, similar to the anatomical structure of the tree rings [44]. Using such a classification, it could be possible to reconstruct seasonal growth conditions (possibly not only climatic ones) over periods of up to millennia.

Another possibility in using the above approach is associated with the reconstruction of the tree-ring growth seasonal kinetics for a long historical perspective. The time scale within each season (calendar dates) cannot be precisely estimated from the tree-ring data due to their variability between individual trees, especially in the middle of the growth season, as demonstrated by Perez-de-Lis et al. [45] (although they were using equal-width sectors of tree ring rather than single tracheids). Nevertheless, the features of the wood's anatomical structure may indicate specific climatic events [46,47]. By measuring the tree-ring anatomy over several centuries, one can determine the repeatability of such indicators, and, therefore, try to determine the likelihood and possible cyclicity of their appearance in the future [48]. Of course, a reconstruction of the growth seasonal kinetics is of particular interest for comparison with the phenology of the annual development cycle in a woody plant [47,49,50]. It is known that different woody plants, including conifers, have their own "clocks" for starting, accelerating, and slowing down seasonal growth [51]. The reconstruction of seasonal kinetics will reveal such features and show evolutionary differences, causing differences between conifers in terms of both their seasonal phenology and their adaptation to changing environmental conditions [49,52]. If such reconstructions can be realized for different conifers growing in the same climatic region, this could help to determine the range of resistance of species to environmental fluctuations, primarily climatic ones. Combining this approach with the first attempts to quantitatively describe



the kinetics of wood formation in angiosperm trees, such as in [53], may also prove to be extremely useful, considering the widespread dominance of broadleaved forests and woody species across the globe.

## 5. Conclusions

The implementation of a complex approach including a combination of the VS-model and the Band-model to imitate the seasonal kinetics of radial growth at different levels (growth rate in general, cell production, and size) proved to fit actual data on both cell population kinetics in the developing ring and final tree-ring structure. Further approbation of this approach on various datasets is required to test its ability to describe wood formation under various limiting factors, and for conifer species with differing ecophysiological strategies and tolerances.

**Supplementary Materials:** The following supporting information can be downloaded at: <https://www.mdpi.com/article/10.3390/f15020249/s1>, Table S1: Characteristics of sampling sites, tree-ring width series and chronologies; Table S2: Tree-ring width (TRW), cell number per radial row (N), and mean cell radial size of tracheids (D) for tree rings formed during years of seasonal kinetics observations, as measured in the last samples, for each particular tree; Table S3: Parameters of VS-model fitted for two sampling sites using VS-oscillograph implementation, and resulting statistical characteristics of the modeling for entire period of simulation; Figure S1: Simulated with VS-model and actual chronologies of the tree-ring width indexes (TRWi) for two sampling sites; Figure S2: Daily mean temperatures and amount of precipitation over season significant for tree growth for years of the seasonal kinetics observation (as determined in VS-model), derived from the Minusinsk station data.

**Author Contributions:** Conceptualization, E.A.V.; methodology, B.Y. and E.A.V.; validation, E.A.B.; formal analysis, G.K.Z., L.V.B. and G.A.S.; investigation, D.F.Z.; resources, E.A.B. and D.F.Z.; data curation, X.P. and J.L.; writing—original draft preparation, all authors; writing—review and editing, L.V.B., B.Y., X.P. and J.L.; visualization, G.K.Z. and L.V.B.; supervision, E.A.V.; project administration, E.A.B. and D.F.Z.; funding acquisition, B.Y. and E.A.V. All authors have read and agreed to the published version of the manuscript.

**Funding:** This research was funded by the Russian Science Foundation, grant no. 23-44-00067, and the National Natural Science Foundation of China, grant no. 42261134537, in the framework of a joint Russian–Chinese project.

**Data Availability Statement:** The data presented in this study are available on request from the corresponding author.

**Conflicts of Interest:** The authors declare no conflicts of interest. The funders had no role in the design of the study; in the collection, analyses, or interpretation of data; in the writing of the manuscript; or in the decision to publish the results.

## References

1. Vaganov, E.A.; Shashkin, A.V.; Sviderskaya, I.V.; Vysotskaya, L.G. *Histometric Analysis of Woody Plants Growth*; Nauka: Novosibirsk, Russia, 1985; 102p. (In Russian)
2. Vaganov, E.A.; Hughes, M.K.; Shashkin, A.V. *Growth Dynamics of Conifer Tree Rings: Images of Past and Future Environments*; Springer: Berlin/Heidelberg, Germany, 2006; 358p. [\[CrossRef\]](#)
3. Rathgeber, C.B.K.; Cuny, H.E.; Fonti, P. Biological basis of tree-ring formation: A crash course. *Front. Plant Sci.* **2016**, *7*, 734. [\[CrossRef\]](#)
4. Rathgeber, C.B.K.; Perez-de-Lis, G.; Fernandez-de-Una, L.; Fonti, P.; Rossi, S.; Treydte, K.; Gessler, A.; Deslaurier, A.; Fonti, M.; Ponton, S. Anatomical, developmental and physiological bases of tree-ring formation in relation to environmental factors. In *Stable Isotopes in Tree Rings: Inferring Physiological, Climatic and Environmental Responses*; Siegwolf, R.T.W., Brooks, J.R., Roden, J., Saurer, M., Eds.; Springer International Publishing: Cham, Switzerland, 2022; pp. 61–99. [\[CrossRef\]](#)
5. Ziaco, E.; Biondi, F.B.; Heinrich, I. Wood cellular dendroclimatology: Testing view proxies in Great Basin bristlecone pine. *Front. Plant Sci.* **2016**, *7*, 1602. [\[CrossRef\]](#)
6. Babushkina, E.A.; Sitnikov, G.A.; Upadhyay, K.K.; Zhirnova, D.F.; Zelenov, G.K.; Vaganov, E.A.; Belokopytova, L.V. Seasonal growth of pine tree rings: Comparison of direct observations and simulation. *Forests* **2022**, *13*, 1978. [\[CrossRef\]](#)

7. Begum, S.; Nakaba, S.; Yamagishi, Y.; Oribe, Y.; Funada, R. Regulation of cambial activity in relation to environmental conditions: Understanding the role of temperature in wood formation of trees. *Physiol. Plant.* **2012**, *147*, 46–54. [[CrossRef](#)] [[PubMed](#)]
8. Begum, S.; Kudo, K.; Rahman, M.H.; Nakaba, S.; Yamagishi, Y.; Nabeshima, E.; Nugroho, W.D.; Oribe, Y.; Kitin, P.; Jin, H.-O.; et al. Climate change and the regulation of wood formation in trees by temperature. *Trees* **2018**, *32*, 3–15. [[CrossRef](#)]
9. Babushkina, E.A.; Belokopytova, L.V.; Zhirnova, D.F.; Vaganov, E.A. Siberian spruce tree ring anatomy: Imprint of development processes and their high-temporal environmental regulation. *Dendrochronologia* **2019**, *53*, 114–124. [[CrossRef](#)]
10. Belokopytova, L.V.; Babushkina, E.A.; Zhirnova, D.F.; Panyushkina, I.P.; Vaganov, E.A. Pine and larch tracheids capture seasonal variations of climatic signal at moisture-limited sites. *Trees* **2019**, *33*, 227–242. [[CrossRef](#)]
11. De Micco, V.; Carrer, M.; Rathgeber, C.B.K.; Camarero, J.; Voltas, J.; Cherubini, P.; Battipaglia, G. From xylogenesis to tree rings: Wood traits to investigate tree response to environmental changes. *IAWA J.* **2019**, *40*, 155–182. [[CrossRef](#)]
12. Butto, V.; Deslaurier, A.; Rossi, S.; Rozenberg, P.; Shishov, V.; Morin, H. The role of plant hormones in tree-ring formation. *Trees* **2020**, *34*, 315–335. [[CrossRef](#)]
13. Deleuze, C.; Houllier, F. A simple process-based xylem growth model for describing wood microdensitometric profiles. *J. Theor. Biol.* **1998**, *193*, 99–113. [[CrossRef](#)]
14. Cuny, H.E.; Rathgeber, C.B.K.; Frank, D.; Fonti, P.; Fournier, M. Kinetics of tracheid development explain conifer tree-ring structure. *New Phytol.* **2014**, *203*, 1231–1241. [[CrossRef](#)]
15. Drew, D.M.; Downes, G. A model of stem growth and wood formation in *Pinus radiata*. *Trees* **2015**, *29*, 1395–1413. [[CrossRef](#)]
16. Hartmann, F.P.K.; Rathgeber, C.B.; Fournier, M.; Moulia, B. Modelling wood formation and structure: Power and limits of a morphogenetic gradient in controlling xylem cell proliferation and growth. *Ann. For. Sci.* **2017**, *74*, 14. [[CrossRef](#)]
17. Hartmann, F.P.; Rathgeber, C.B.K.; Badel, E.; Fournier, M.; Moulia, B. Modelling the spatial crosstalk between two biochemical signals explains wood formation dynamics and tree-ring structure. *J. Exp. Bot.* **2021**, *72*, 1727–1737. [[CrossRef](#)] [[PubMed](#)]
18. Carteni, F.; Deslauriers, A.; Rossi, S.; Morin, H.; De Micco, V.; Mazzoleni, S.; Giannino, F. The physiological mechanisms behind the earlywood-to-latewood transition: A process-based modeling approach. *Front. Plant Sci.* **2018**, *9*, 1053. [[CrossRef](#)] [[PubMed](#)]
19. Tychkov, I.I.; Sviderskaya, I.V.; Babushkina, E.A.; Popkova, M.I.; Vaganov, E.A.; Shishov, V.V. How can the parameterization of a process-based model help us understand real tree-ring growth? *Trees* **2019**, *33*, 345–357. [[CrossRef](#)]
20. Cabon, A.; Peters, R.L.; Fonti, P.; Martínez-Vilalta, J.; Cáceres, M.D. Temperature and water potential co-limit stem cambial activity along a steep elevational gradient. *New Phytol.* **2020**, *226*, 1325–1340. [[CrossRef](#)] [[PubMed](#)]
21. Eckes-Shepard, A.H.; Ljungqvist, F.C.; Drew, D.M.; Rathgeber, C.B.K.; Friend, A.D. Wood formation modeling—A research review and future perspectives. *Front. Plant Sci.* **2022**, *13*, 837648. [[CrossRef](#)]
22. Shishov, V.V.; Tychkov, I.I.; Anchukaitis, K.J.; Zelenov, G.K.; Vaganov, E.A. A band model of cambium development: Opportunities and prospects. *Forests* **2021**, *12*, 1361. [[CrossRef](#)]
23. Seo, J.W.; Smiljanić, M.; Wilmking, M. Optimizing cell-anatomical chronologies of Scots pine by stepwise increasing the number of radial tracheid rows included—Case study based on three Scandinavian sites. *Dendrochronologia* **2014**, *32*, 205–209. [[CrossRef](#)]
24. Shishov, V.V.; Tychkov, I.I.; Popkova, M.I.; Ilyin, V.A.; Bryukhanova, M.V.; Kirilyanov, A.V. VS-Oscilloscope: A new tool to parameterize tree radial growth based on climate conditions. *Dendrochronologia* **2016**, *39*, 42–50. [[CrossRef](#)]
25. Anchukaitis, K.J.; Evans, M.N.; Hughes, M.K.; Vaganov, E.A. An interpreted language implementation of the Vaganov-Shashkin tree-ring proxy system model. *Dendrochronologia* **2020**, *60*, 125677. [[CrossRef](#)]
26. Fonti, M.V.; Babushkina, E.A.; Zhirnova, D.F.; Vaganov, E.A. Xylogenesis of Scots pine in an uneven-aged stand of the Minusinsk Depression (Southern Siberia). *J. Sib. Fed. Univ. Biol.* **2020**, *13*, 197–207. [[CrossRef](#)]
27. Cook, E.R.; Kairiukstis, L.A. (Eds.) *Methods of Dendrochronology: Applications in the Environmental Sciences*; Kluwer Acad. Publ.: Dordrecht, The Netherlands, 1990. [[CrossRef](#)]
28. Rinn, F. *TSAP-Win: Time Series Analysis and Presentation for Dendrochronology and Related Applications: User Reference*; RINNTECH: Berlin/Heidelberg, Germany, 2003.
29. Holmes, R.L. Computer-assisted quality control in tree-ring dating and measurement. *Tree-Ring Bull.* **1983**, *43*, 69–78.
30. Cook, E.R.; Krusic, P.J. *Program ARSTAN: A Tree-Ring Standardization Program Based on Detrending and Autoregressive Time Series Modeling, with Interactive Graphics*; Lamont-Doherty Earth Observatory, Columbia University: Palisades, NY, USA, 2005.
31. Vysotskaya, L.G.; Vaganov, E.A. Components of the variability of radial cell size in tree-rings of conifers. *IAWA Bull.* **1989**, *10*, 417–428. [[CrossRef](#)]
32. Vaganov, E.A.; Ivanov, V.B.; Vysotskaya, L.G. Histometric analysis of cell size variability in the meristem of corn root. *Tsytologya* **1991**, *33*, 50–59. (In Russian)
33. Rossi, S.; Deslauriers, A.; Gričar, J.; Seo, J.W.; Rathgeber, C.B.; Anfodillo, T.; Morin, H.; Levanic, T.; Oven, P.; Jalkanen, R. Critical temperatures for xylogenesis in conifers of cold climates. *Glob. Ecol. Biogeogr.* **2008**, *17*, 696–707. [[CrossRef](#)]
34. Russell, M.B.; Weiskittel, A.R.; Kershaw, J.A., Jr. Assessing model performance in forecasting long-term individual tree diameter versus basal area increment for the primary Acadian tree species. *Can. J. For. Res.* **2011**, *41*, 2267–2275. [[CrossRef](#)]
35. Deslaurier, A.; Morin, H.; Begin, Y. Cellular phenology of annual ring formation of *Abies balsamea* in the Quebec boreal forest (Canada). *Can. J. For. Res.* **2003**, *33*, 190–200. [[CrossRef](#)]
36. Cabon, A.; Fernandez-de-Una, L.; Gea-Izquierdo, G.; Meinzer, F.C.; Woodruff, D.R.; Martínez-Vilalta, J.; De Cáceres, M. Water potential control of turgor-driven tracheid enlargement in Scots pine at its xeric distribution edge. *New Phytol.* **2020**, *225*, 209–221. [[CrossRef](#)]

37. Peters, R.L.; Steppe, K.; Cuny, H.E.; De Pauw, D.J.W.; Frank, D.C.; Schaub, M.; Rathgeber, C.B.K.; Cabon, A.; Fonti, P. Turgor—A limiting factor for radial growth in mature conifers along an elevational gradient. *New Phytol.* **2021**, *229*, 213–229. [[CrossRef](#)]
38. Vaganov, E.A. The tracheidogram method in tree-ring analysis and its application. In *Methods of Dendrochronology: Applications in the Environmental Sciences*; Cook, E., Kairiukstis, L., Eds.; Kluwer Academic Publishers: Dordrecht, The Netherlands, 1990; pp. 63–75.
39. Vaganov, E.A.; Anchukaitis, K.J.; Evans, M. How well understood are the processes that create dendroclimatic records? A mechanistic model of the climatic control on conifer tree-ring growth dynamics. In *Dendroclimatology: Progress and Prospects*; Hughes, M.K., Swetnam, T.W., Diaz, H.F., Eds.; Springer: Dordrecht, Germany, 2011; pp. 37–75. [[CrossRef](#)]
40. Ziaco, E.; Truettner, C.; Biondi, F.; Bullock, S. Moisture-driven xylogenesis in *Pinus ponderosa* from a Mojave desert mountain reveals high phenological plasticity. *Plant Cell Environ.* **2018**, *41*, 823–836. [[CrossRef](#)] [[PubMed](#)]
41. Cuny, H.E.; Rathgeber, C.B.; Frank, D.; Fonti, P.; Mäkinen, H.; Prislán, P.; Rossi, S.; Martínez del Castillo, E.; Campelo, F.; Vavřík, H.; et al. Woody biomass production lags stem-girth increase by over one month in coniferous forests. *Nat. Plants* **2015**, *1*, 15160. [[CrossRef](#)] [[PubMed](#)]
42. Anchukaitis, K.J.; Evans, M.N.; Kaplan, A.; Vaganov, E.A.; Hughes, M.K.; Grissino-Mayer, H.D.; Cane, M.A. Forward modeling of regional scale tree-ring patterns in the southeastern United States and recent influence of summer drought. *Geophys. Res. Lett.* **2006**, *33*, L04705. [[CrossRef](#)]
43. Osakabe, Y.; Kajita, S.; Osakabe, K. Genetic engineering of woody plants: Current and future targets in a stressful environment. *Physiol. Plant* **2011**, *142*, 105–117. [[CrossRef](#)] [[PubMed](#)]
44. Zharkov, M.S.; Huang, J.G.; Yang, B.; Babushkina, E.A.; Belokopytova, L.V.; Vaganov, E.A.; Zhirnova, D.F.; Ilyin, V.A.; Popkova, M.A.; Shishov, V.V. Tracheidograms classification as a new potential proxy in high-resolution dendroclimatic reconstruction. *Forests* **2022**, *13*, 970. [[CrossRef](#)]
45. Perez-de-Lis, G.; Rathgeber, C.B.; Fernández-de-Uña, L.; Ponton, S. Cutting tree rings into time slices: How intra-annual dynamics of wood formation help decipher the space-for-time conversion. *New Phytol.* **2022**, *233*, 1520–1534. [[CrossRef](#)] [[PubMed](#)]
46. Wimmer, R. Wood anatomical features in tree-rings as indicators of environmental change. *Dendrochronologia* **2002**, *20*, 21–36. [[CrossRef](#)]
47. Brauning, A.; De Ridder, M.; Zafirov, N.; García-González, I.; Dimitrov, D.P.; Gärtner, H. Tree-ring features: Indicators of extreme event impacts. *IAWA J.* **2016**, *37*, 206–231. [[CrossRef](#)]
48. Fritts, H.C. Dendroclimatology and dendroecology. *Quat. Res.* **1971**, *1*, 419–449. [[CrossRef](#)]
49. Prislán, P.; Gricar, J.; de Luis, M.; Novak, K.; Martínez del Castillo, E.; Schmitt, U.; Koch, G.; Strus, J.; Mrak, P.; Znidaric, M.T.; et al. Annual cambial rhythm in *Pinus halepensis* and *Pinus sylvestris* as indicator for climatic adaptation. *Front. Plant Sci.* **2016**, *7*, 1923. [[CrossRef](#)] [[PubMed](#)]
50. Carrer, M.; Castagneri, D.; Prendin, A.L.; Petit, G.; von Arx, G. Retrospective analysis of wood anatomical traits reveals a recent extension in tree cambial activity in two high-elevation conifers. *Front. Plant. Sci.* **2017**, *8*, 737. [[CrossRef](#)] [[PubMed](#)]
51. Barlow, P.W.; Lück, J. Repetitive cellular patterns in the secondary phloem of conifer and dicot trees, and a hypothesis for their development. *Plant Biosyst. Int. J. Deal. Asp. Plant Biol.* **2005**, *139*, 164–179. [[CrossRef](#)]
52. Tumajer, J.; Buras, A.; Camarero, J.J.; Carrer, M.; Shetti, R.; Wilmking, M.; Altman, J.; Sangüesa-Barreda, G.; Lehejček, J. Growing faster, longer or both? Modelling plastic response of *Juniperus communis* growth phenology to climate change. *Glob. Ecol. Biogeogr.* **2021**, *30*, 2229–2244. [[CrossRef](#)]
53. Noyer, E.; Stojanovic, M.; Horacek, P.; Perez-de-Lis, G. Toward a better understanding of angiosperm xylogenesis: A new method for a cellular approach. *New Phytol.* **2023**, *239*, 792–805. [[CrossRef](#)]

**Disclaimer/Publisher’s Note:** The statements, opinions and data contained in all publications are solely those of the individual author(s) and contributor(s) and not of MDPI and/or the editor(s). MDPI and/or the editor(s) disclaim responsibility for any injury to people or property resulting from any ideas, methods, instructions or products referred to in the content.